# USING REMOTE SENSING PRODUCTS FOR ENVIRONMENTAL ANALYSIS IN SOUTH AMERICA

Y. E. Shimabukuro [a, *], G. Pereira [a], G. B. S. Silva [a], F. B. Silva [a], F. S. Cardozo [a], E. C. Moraes [a]

[a] INPE, Instituto Nacional de Pesquisas Espaciais, Brazil (yosio, gabriel, bayma, fabricio, cardozo, bete)@dsr.inpe.br

**KEY WORDS:** Land use, land cover, GLOBCOVER, vegetation cover fraction, fire radiative power, biomass burning.

ABSTRACT: Land cover plays a major role in many biogeochemical models that represent processes and connections with terrestrial systems; hence, it is a key component for public decisions in ecosystems management. The advance of remote sensing technology, combined with the emergence of new operational products, offers alternatives to improve the accuracy of environmental monitoring and analysis. This work uses four remotely sensed databases: the GLOBCOVER, the Vegetation Continuous Field (VCF), MODIS Fire Radiative Power (FRP) and the Tropical Rainfall Measuring Mission (TRMM). The objective of this study is to analyze the environmental characteristics in South America from 2000 to 2005 using these four remotely sensed databases. Initially, GLOBCOVER was assessed based on VCF product, and was afterwards analyzed for its quantitative and spatial distribution of the fires with the FRP database. The results show that GLOBCOVER has a tendency to overestimate forest classes and to underestimate urban and mangroves areas. The fire quantification on GLOBCOVER product shows that the highest incidence of fires can be observed in the deforestation arc, located in the Amazon forest border, with vegetation cover composed mainly of broadleaved evergreen or semi-deciduous forest. A time series analysis of FRP database indicates that biomass burning spreads to areas of broadleaved evergreen or semi-deciduous forest and savannah regions, even with rainfall anomalies observed with TRMM database. We suggest to improve the map of vegetation and urban areas and to use other products derived from satellites, such as the images of City Lights, created out of data from the Defence Meteorological Satellite Program (DMSP).

## 1. INTRODUCTION

Land cover plays a major role in many environmental models that represent processes and connections between surface and atmospheric processes, which modify the energy balance (Kaufman et al., 1998; Christopher et al., 1998; Tarasova et al., 1999; Tarasova et al., 2000; Tarasova & Eck, 2000; Christopher et al., 2000; Li et al., 2000; Wagner et al., 2001), atmospheric chemistry (Crutzen & Andreae, 1990; Fishman et al., 1996; Reid et al., 1996, 1999), evapotranspiration and precipitation reduction (Nobre et al., 1991, 1998). Hence, land cover is a key component for public decisions on ecosystems management and in the assessment of the impacts of anthropogenic actions on the equilibrium of ecosystems.

Overtime, biomass burning consumes vast areas of grassland and forests around the globe, releasing large and unknown quantities of aerosols and trace gases into the atmosphere (Crutzen & Andreae, 1990). In South America, land use and land cover (LULC) maps show temporal and spatial variability in anthropogenic biomass burning, which are directly associated with agricultural land clearing, grassland management and with the deforestation of Amazon tropical rainforest, the highest incidences of fires are located in the arc of deforestation, located in Amazon forest border (Kaufman et al., 1990, 1992).

The GLOBCOVER project is an initiative of European Space Agency (ESA) in cooperation with international institutions; it is useful in monitoring the dynamics of land cover and forests (Arino et al., 2005). The EOS (Earth Observing System) initiative of NASA **(**National Aeronautics and Space Administration) is another program that provides important data for environmental monitoring of land, ocean and atmospheric ecosystems.

Among the many products provided by the EOS, the VCF (Vegetation Continuous Field) and the MODIS (Moderate Imaging Spectroradiometer) provide phenological studies in annual time series (Hansen et al., 2003).

Despite the efforts of each program in implementing environmental, hardware, software and data distribution, these aforementioned products have their respective limitations and are creating confusion in distinguishing the different classes of land cover (Herold et al., 2008).

Integration of different data sources from different sensors can improve the accuracy of environmental monitoring. Thus, the objective of this study is to verify GLOBCOVER LULC product assessment with VCF tree cover data. Furthermore, using MODIS data, the patterns of fire radiative power over LULC and VCF values are compared by analysing the annual biomass burning distribution in South America from 2000 to 2005.

## 2. DATA AND METHODOLOGY

### 2.1 GLOBCOVER

Figure 1 shows South America GLOBCOVER product. South America has a distinct and important biodiversity in the world, spatially distributed in its many natural ecosystems. However, this complex system is constantly exposed to anthropogenic activities such as deforestation, agriculture expansion and burning.

The objective of the ESA-GLOBCOVER project is the production of a land cover map of the world using an automated processing chain on 300m MERIS time series. The GLOBCOVER Land Cover map for the period of December

* Corresponding author.

2004 to June 2006 is derived by an automatic and regionally-tuned classification of a MERIS full resolution (FR) time series. Its 22 land cover classes are defined with the UN Land Cover Classification System (LCCS).

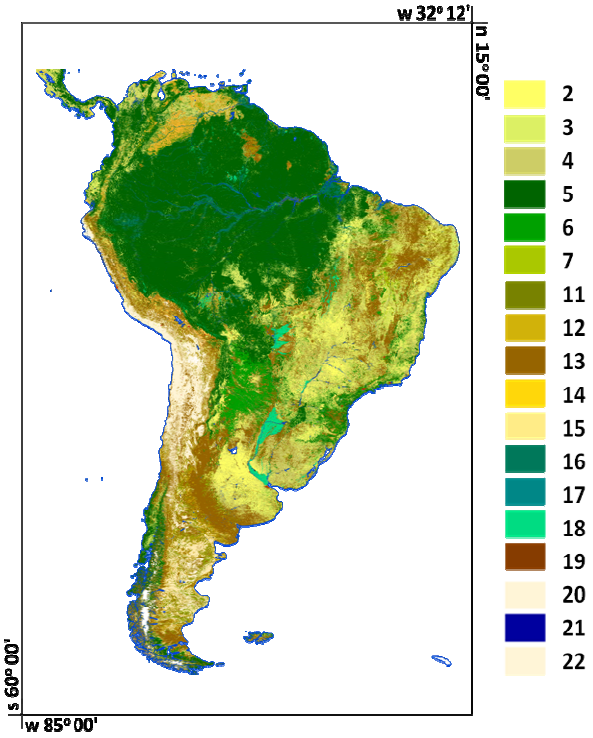


Figure 1. GLOBCOVER product of South America.

In South America (Figure 1) the following classes are found: 2 - Rainfed croplands; 3 - Mosaic cropland (50-70%) / vegetation (grassland/shrubland/forest) (20-50%); 4 - Mosaic vegetation (grassland/shrubland/forest) (50-70%) / cropland (20-50%); 5 - Closed to open (>15%) broadleaved evergreen or semi-deciduous forest (>5m); 6 - Closed (>40%) broadleaved deciduous forest (>5m); 7 - Open (15-40%) broadleaved deciduous forest/woodland (>5m); 8 - Closed (>40%) needleleaved evergreen forest (>5m); 9 - Open (15-40%) needleleaved deciduous or evergreen forest (>5m); 10 -Closed to open (>15%) mixed broadleaved and needleleaved forest (>5m); 11 - Mosaic forest or shrubland (50-70%) / grassland (20-50%); 12 - Mosaic grassland (50-70%) / forest or shrubland (20-50%); 13 - Closed to open (>15%) (broadleaved or needleleaved, evergreen or deciduous) shrubland (<5m); 14 - Closed to open (>15%) herbaceous vegetation (grassland, savannas or lichens/mosses); 15 - Sparse (<15%) vegetation; 16 - Closed to open (>15%) broadleaved forest regularly flooded (semi-permanently or temporarily) - Fresh or brackish water; 17 - Closed (>40%) broadleaved forest or shrubland permanently flooded - Saline or brackish water; 18 - Closed to open (>15%) grassland or woody vegetation on regularly flooded or waterlogged soil - Fresh, brackish or saline water; 19 - Artificial surfaces and associated areas (Urban areas >50%); 20 - Bare areas; 21 - Water bodies; 22 - Permanent snow and ice; and 23 - No data (burnt areas, clouds,…) (Bicheron et al., 2009).

### 2.2 Vegetation Continuous Fields (VCF)

The Vegetation Continuous Fields (VCF) (Figure 2) is a global percent tree cover map based on 500 meter MODIS data, and represents the finest scale global forest information to date. In this study, the MODIS composited data are transformed into annual metrics which capture the salient points in the forest phenologic cycle. The VCF algorithm is an automated procedure which employs a regression tree algorithm. Percent canopy here refers to the amount of skylight obstructed by tree canopies which are equal to or greater than 5 meters in height (Hansen et al., 2003).

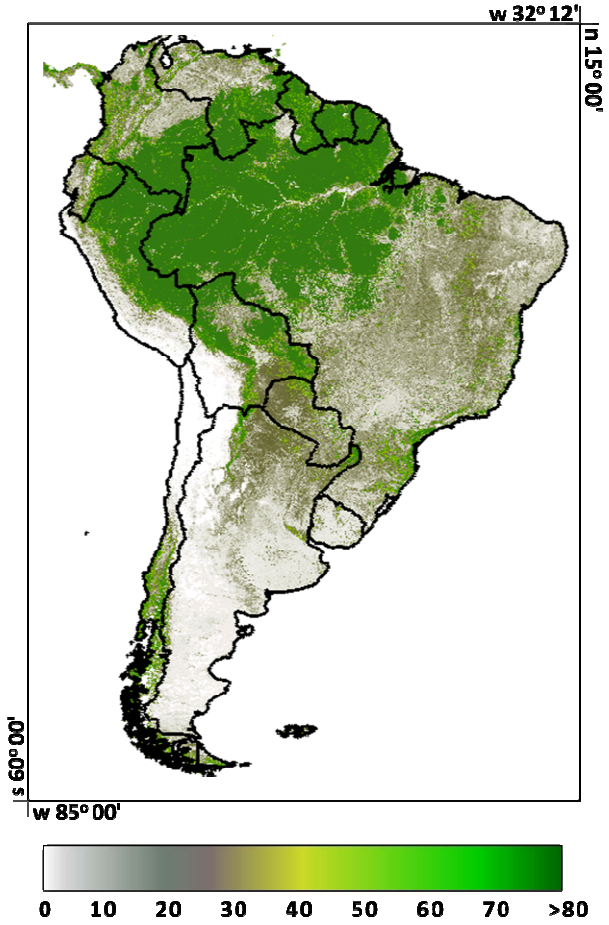


Figure 2. 2005 South America Vegetation Continuous Fields product.

### 2.3 Tropical Rainfall Measuring Mission (TRMM)

The TRMM satellite data are used in this study to characterize the seasonal pattern of precipitation. The TRMM satellite is a partnership between the National Aeronautics and Space Administration (NASA) and the Japan Aerospace Exploration Agency (JAXA). Since 1997, these agencies have collected precipitation data encompassing more than two thirds of global precipitation. These data are generated by an algorithm that estimates the combined global precipitation estimations from multiple orbital sensors (Huffman et al., 2007). The data used in this work are related to the 3B42 product with 3 hours of temporal resolution; geographic covering: latitude from 50° S to 50° N and longitude from 180°W to 180°E; and horizontal resolution of 0.25° x 0.25° (available in: <http://mirador.gsfc.nasa.gov/>).

### 2.4 MODIS Fire Radiative Power (FRP)

The fraction of chemical energy emitted in biomass burning as electromagnetic radiation can be defined as Fire Radiative Power (FRP). Temporal integration of FRP gives the Fire Radiative Energy (FRE). Moreover, the FRE indicates the

amount of particulate matter and trace gases emitted into the atmosphere over a region (Pereira et al., 2009). Initial studies with FRP were performed with MODIS Airborne Simulator (MAS) in the SCAR-C and SCAR-B (Smoke, Cloud and Radiation - California / Brazil) experiments are available on MODIS fire products, also called MOD14 (Terra) and MYD14 (Aqua); these products utilizes a contextual algorithm applied to brightness temperatures in 4 µm and 11 µm mid-infrared radiation channels (Kaufman et al., 1998a, 1998b; Chu et al., 1998; Justice et al., 2002; Giglio, 2005) and for each fire detection FRP is calculated through the method proposed by Kaufman et al. (1996, 1998a, 1998b):

$$FRP_{MODIS} = 4.3x10^{-19} . (T^{8}_{f\,4\mu m} - T^{8}_{b\,4\mu m}) . A_{sampl} \quad (1)$$

where $T_f$ 4µm and $T_b$ 4µm are, respectively, the MODIS brightness temperatures of the fire and the non-fire background in Kelvin (K), $A_{sampl}$ is the real area of the pixel (m) and FRP is the Fire Radiative Power in Megawatts (MW) as shown for the 2005 fire data (Figure 3).

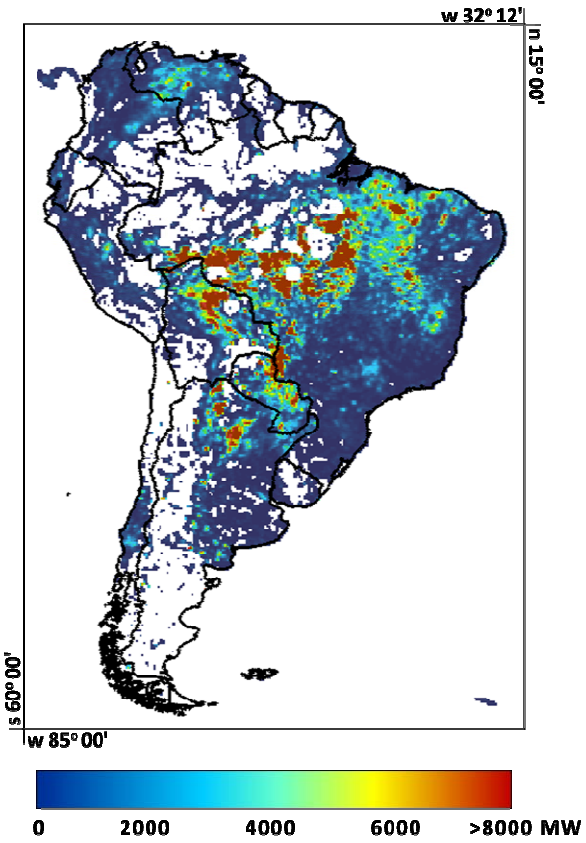


Figure 3. 2005 South America MODIS FRP product.

### 2.5 Data processing

All data used in this work are inserted in SPRING, a free GIS application developed by the National Institute for Space Research (INPE) of the Brazilian Ministry of Science and Technology (MCT). Part of the data processing stage (transformation and compilation of different data, random sampling, assignment of thematic classes and cross tabulation analysis) was made in LEGAL Language implemented in the SPRING (SPRING, 2005). LEGAL is a command language used to geographic analysis that is not implemented on graphic interface of SPRING. This command language, proposed by Câmara Neto (1995), has as objective to support a command line tool to perform spatial queries operations and numerical and statistical analysis.

Figure 4 shows the flowchart of the adopted methodology. The first step (I) consists in acquire remote sensing derived products; follow by data processing and SPRING data base inclusion (II). After this step, derived data was compared in pairs (III) and the results analyzed (IV).

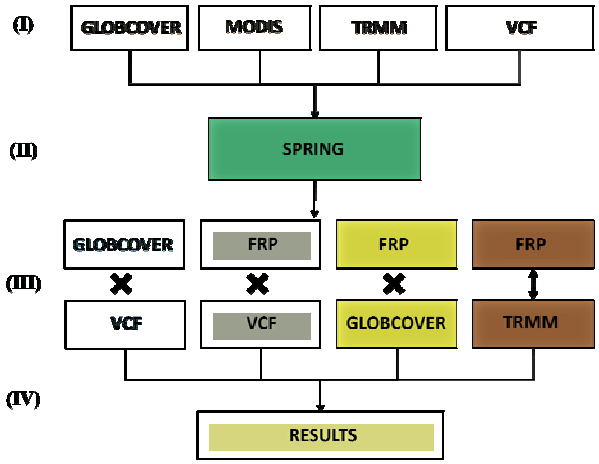


Figure 4. Flowchart of methodology.

## 3. RESULTS

### 3.1 GLOBCOVER assessment with VCF

GLOBCOVER product characterizes South America LULC in 19 classes, which represents approximately 40% broadleaved evergreen or semi-deciduous forest such as Amazon forest and Atlantic Forest (tropical and subtropical moist forest), 17% are a merger of vegetation and cropland, 16% represents closed to open broad-leaved or needle-leaved, evergreen or deciduous shrubland and 6% is rainfed croplands. Also, there are minority class areas such as bare areas (3%), Sparse Vegetation (3%) and Grassland/Shrubland Forest (9%).

Operational landscape characterization methodologies could introduce systematic errors due to surface elements with spectral signature similarities (Wang & Howarth, 1993). Consequently, remote sensing derived products such as VCF could be used to assess LULC maps. Figure 5 shows the cross tabulation between the mainly LULC South America GLOBCOVER classes and 2005 VCF tree cover product. Broad-leaved evergreen or semi-deciduous forest land cover, mainly represented by Amazon Rainforest, are expected to have a high value of VCF tree cover due to the large area of vast forests that perform homogeneous tree cover. However, the results showed that only approximately 72% of the total LULC area is composed of VCF values greater than 70. The same occurs with Closed broadleaved deciduous forest, located essentially in Paraguay and North of Argentina, where approximately 40% of this class area are composed of VCF tree cover lower than 40.

This discrepancy could be originated by the heterogeneity of vegetation on pixel formation. In this area, we can found mixed areas of short grass, tall grass, Evergreen broadleaf trees and

Forest-Field Mosaic that introduces errors in classification process.

However, LULC classes dominated mainly by agricultural and grassland fields show good conformity with VCF values, with low percentage (less than 5%) of VFC values greater than 70.

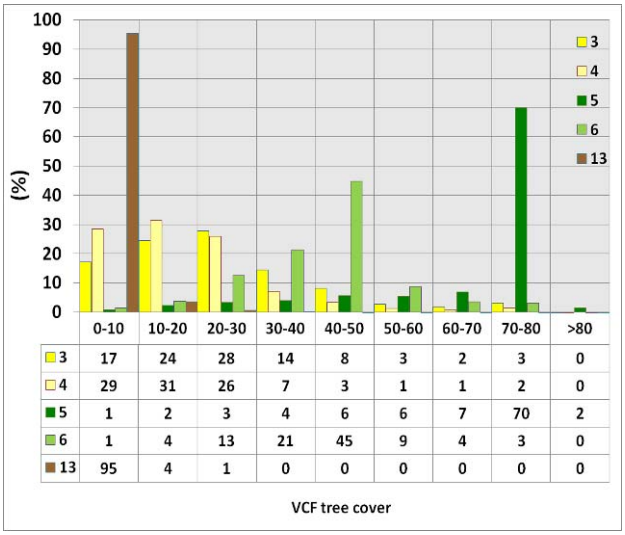


| | 0-10 | 10-20 | 20-30 | 30-40 | 40-50 | 50-60 | 60-70 | 70-80 | >80 |
|---|---|---|---|---|---|---|---|---|---|
| 3 | 17 | 24 | 28 | 14 | 8 | 3 | 2 | 3 | 0 |
| 4 | 29 | 31 | 26 | 7 | 3 | 1 | 1 | 2 | 0 |
| 5 | 1 | 2 | 3 | 4 | 6 | 6 | 7 | 70 | 2 |
| 6 | 1 | 4 | 13 | 21 | 45 | 9 | 4 | 3 | 0 |
| 13 | 95 | 4 | 1 | 0 | 0 | 0 | 0 | 0 | 0 |

Figure 5. Graphic of cross tabulation between GLOBCOVER and VCF products, showing the percentage of vegetation continuous field tree cover present in selected land use and land cover map.

GLOBCOVER product exhibits a tendency to overestimate forest classes mainly by clustering surrounding lower biomass density LULC areas such as shrubland and grassland. Also, we can notice that it underestimates urban areas and mangroves biome. These errors, associated with the algorithm classifier, could be introduced in the pre-processing of MERIS imagery, in the radiometric rectification and in cloud-free processing algorithm. Figure 6 shows a sample area with broad-leaved evergreen forest LULC GLOBCOVER (in dark green) with the respective VCF tree cover product and MODIS True color composition (3B4G1R) cloud-free mosaic sections, (a), (b) and (c), respectively. This figure is an example of the over-estimation that occurs in LULC product.

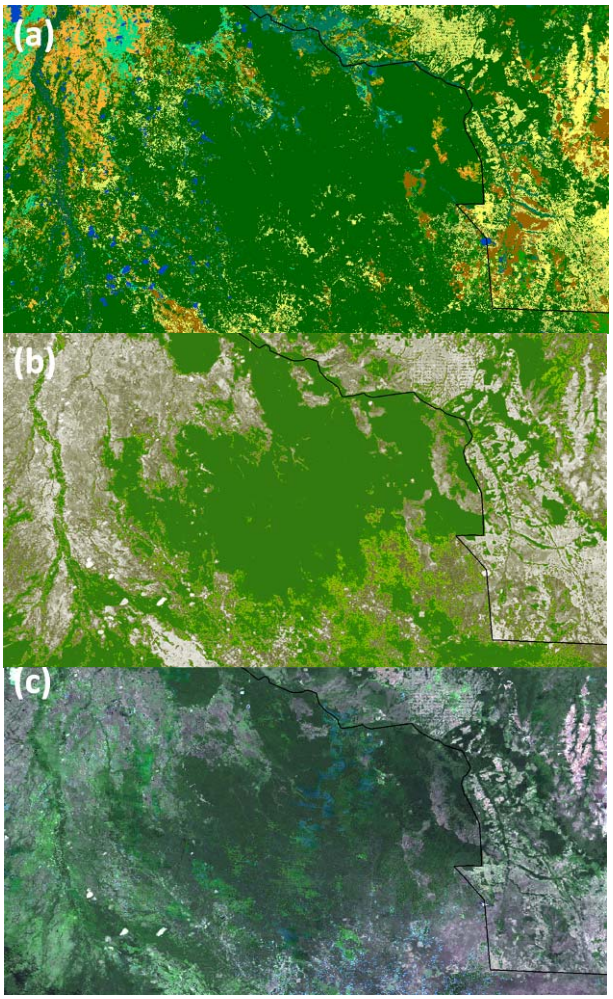


Figure 6. (a) Example of Closed to open (>15%) broadleaved evergreen or semi-deciduous forest (>5m) overestimation (in dark green); (b) VCF tree cover; and (c) MODIS surface reflectance composition (3B4G1R).

### 3.2 2000 to 2005 South America Biomass Burning

In South America, biomass burning presents spatial and temporal variability, associated directly with LULC management. The highest incidences of fires are located in the arc of deforestation, located in the Amazon forest borders. Therefore, the greatest number of fires can be found in areas of vegetation composed by broad-leaved evergreen or semi-deciduous forest; this is followed by herbaceous vegetation (grassland, savannas or lichens/mosses); mosaic vegetation (grassland /shrubland/forest) / cropland; mosaic cropland / vegetation (grassland/shrubland/forest) and rainfed croplands. Table 1 shows the LULC for South America and its percentage of 2005 fires presented in each class.

| GLOBCOVER LULC | (%) |
|---|---|
| 2 | 6.4 |
| 3 | 7.8 |
| 4 | 9.3 |
| 5 | 38.9 |
| 6 | 3.8 |
| 7 | 0.5 |
| 11 | 3.2 |
| 12 | 1.5 |
| 13 | 16.6 |
| 14 | 2.0 |
| 15 | 3.3 |
| 16 | 1.6 |
| 17 | 0.1 |
| 18 | 1.4 |
| 19 | 0.1 |
| 20 | 3.1 |
| 22 | 0.4 |

Table 1. GLOBCOVER LULC and the percentage of 2005 fires presented in each class.

Figure 7 shows the annual (2000 to 2005) accumulative fire pixels that occur in each VCF tree cover classes (y-axis in logarithm of base 10). We can notice that most of South America´s biomass burning is located in VCF tree cover classes of, 0-10, 20-30 and 70-80. Also, this figure shows a propensity to increasing the number of fire focus in all VCF classes, mainly in VCF values greater than 70, that represents biomes with a high quantity of biomass. When comparing 2005 to 2000, notice that biomass burning spread to areas of Broad-leaved evergreen or semi-deciduous forest and savannah regions. These areas are composed mainly of Amazon Forest biome and Brazilian Cerrado (savannah biome). Also, the highest increase occurs in vegetation whit continuous field tree cover greater than 79% due the deforestation expansion.

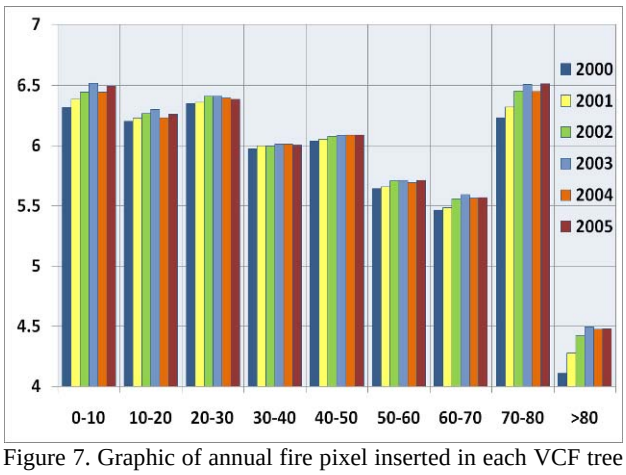


Figure 7. Graphic of annual fire pixel inserted in each VCF tree cover class (values are in logarithm base 10).

Figure 8 shows the annual fire radiative power released per pixel as retrieved from MODIS. This product gives information of active fires 4 to 5 times per day for the same area. The FRP values are clustered in 10km grid, where the pixel value is the sum of all-year FRP values. The highest annual occurrence are detected between 0-1000 MW, in this class we notice a low variation of FRP among the yearly measurements. In the other classes the number of FRP pixels increased significantly especially in values greater than 6000 MW.

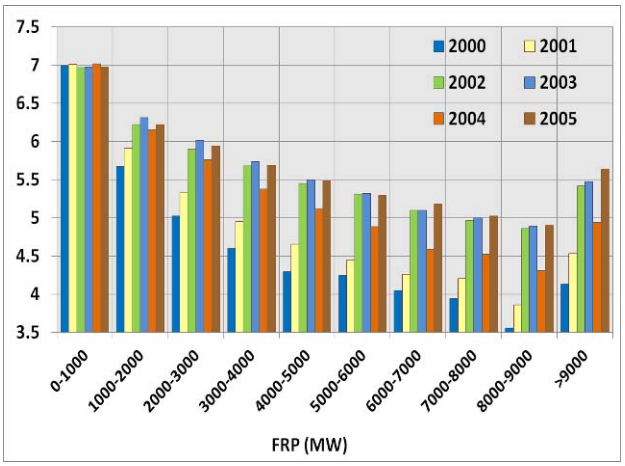


Figure 8. Graphic of annual fire radiative power (in Megawatts) with y-axis in logarithm base 10.

Some variations in FRP clusters can be attributed to the rainfall anomalies, such as in 2004, when South America had a positive anomaly rainfall analysed by TRMM data. During the studied period (2000 to 2005), Amazon region had negative rainfall anomalies in 2002, 2003 and 2005 and positive rainfall anomalies in 2000, 2001 and 2004. Moreover, the increase in energy released by South American fires could be related to increasing of biomass burning in areas with large amounts of biomass exposed annually to anthropogenic burning located in the arc of deforestation (as shown in Figure 3). Figure 9 shows the rainfall anomaly for 2004 derived from TRMM rainfall data.

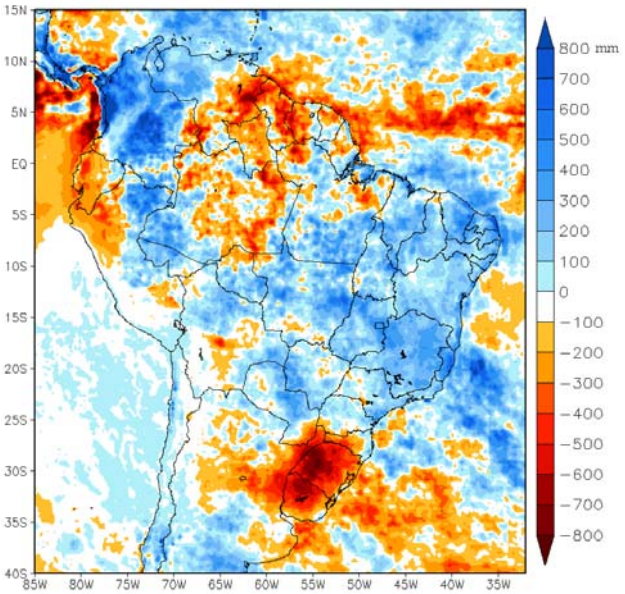


Figure 9. 2004 Rainfall Anomaly, blue represents positive values of rainfall and red represents negative rainfall values.

## 4. CONCLUSIONS

Although GLOBCOVER is a global product, it proved effective in representing the land use and land cover (LULC) of the region. However, like all products derived from automatic classification, some errors present in the results, such as the overestimation of broad-leaved evergreen or semi-deciduous forest and the under-estimation of urban areas and vegetation composed by mangroves. Therefore, to improve the map of vegetation areas and urban areas, we suggest verification using other products derived from satellites, such as the images of City Lights, created with the data from the Defence Meteorological Satellite Program (DMSP).

Concerning the burned areas, it is noticeable that classes with the largest number of fires are related to the Amazon Forest and Cerrado (savannah) biomes and there was a significant increase in the number of fires in areas with a large amount of biomass, resulting therefore in a larger number of emissions of aerosols and trace gases into the atmosphere.

## 5. REFERENCES

Arino, O. et al., 2005. The GLOBCOVER Initiative, ESA ESRIN, Via Galilleo Galilei, Frascati, Italy.

Bicheron, P., Defourny, P., Brockmann, C., Schouten, L., Vancutsem, C., Huc, M., Bontemps, S., Leroy, M., Achard, F., Herold, M., Ranera, F., Arino, O., 2009. GLOBCOVER-Products Description and Validation Report. 47p. Available at: <ftp://guestglobcover:Pir8Eefo@usextnas.eo.esa.int/global/GLOBCOVER.Products_Description_Validation_Report_I2.1.pdf>. Accessed on: 18 Nov 2009.

Câmara Neto, G., 1995. Modelos, linguagens e arquiteturas para banco de dados geográficos. [Tese de Doutorado]. Instituto Nacional de Pesquisas Espaciais..

Christopher, S. A.; Wang, M.; Berendes, T. A.; Welch, R. M., 1998. The 1985 biomass burning season in South America: Satellite Remote Sensing of fires, smoke and regional radiative energy budget. J. Appl. Meteorol., 37, 661-678.

Christopher, S. A.; Li, X.; Welch, R. M.; Reid, J. S.; Hobbs, P. V.; Eck, T. F.; Holben, B., 2000. Estimation of downward and top-of-atmosphere Shortwave Irradiances in Biomass Burning Regions during SCAR-B. Journal of Applied Meteorology, v. 39, n.10, p.1742-1753, Out.

Chu, D. A., Kaufman, Y. J., Remer, L. A., Holben, B. N., 1998. Remote sensing of smoke from MODIS airborne simulator during the SCAR-B experiment. *J. Geophys. Res*., 103, 31, 979-31, 987.

Crutzen, P. J.; Andreae, M. O., 1990. Biomass Burning in the Tropics: Impact on Atmospheric Chemistry and Biogeochemical Cycles. *Science* 250 (4988): 1669-1678.

Fishman, J.; Hoell, J. M.; Bendura, J. R.; Mcneal, R. J.; Kirchhoff, V. W. J. H., 1996. NASA GTE TRACE-A experiment (September-October, 1992). Overview. Journal of Geophysical Research – Atmospheres, v.101, n. D19, p. 23865-23880.

Giglio, L., 2005. MODIS Collection 4 Active Fire Product User's Guide. Available on the Internet: http://maps.geog.umd.edu/products/MODIS_Fire_Users_Guide_2.1.pdf .

Hansen, M. C.; Defries, R. S.; Townshend, J. R. G.; Carroll, M.; Dimiceli, C.; Sohlberg, R. A., 2003. Global Percent Tree Cover at a Spatial Resolution of 500 Meters: First Results of the MODIS Vegetation Continuous Fields Algorithm. *Earth Interactions*, v. 7, n. 10, p. 1-15.

Herold, M., Mayaux, P., Woodcock, C. E., Baccini, A., Schmullius, C., 2008. Challenges in global land cover mapping: an assessment of agreement and accuracy in existing 1km datasets, *Remote Sensing of Environment* 112: 2538-2556.

Huffman, G. J., Adler, R. F., Bolvin, D. T., Gu, G., Nelkin, E. J., Bowman, K. P., Hong, Y., Stocker, E. F., Wolff, D. B., 2007. The TRMM Multi-satellite Precipitation Analysis (TMPA): Quasi-Global, Multiyear, Combined-Sensor Precipitation Estimates at Fine Scale. *Journal of Hydrometeorology*, v. 8, p. 38-55, Feb.

Justice, C. O., Giglio, B., Korontzi, S., Owens, J., Morisette, J. T., Roy, D. P., Descloitres, J., Alleaume, S., Petitcolin, F., Kaufman, Y., 2002. The MODIS fire products. *Remote Sensing of Environment*, 83, 244-262.

Kaufman, Y. J., Tucker, C. J., Fung, I., 1990. Remote Sensing of Biomass Burning in the Tropics. *Journal of Geophysical Research*, v. 95, n. D7, 9927-9939.

Kaufman, Y. J.; Setzer, A. W.; Ward, D.; Tanré, D.; Holben, B. N.; Menzel, P.; Pereira, M. C.; Rasmussen, R., 1992. Biomass Burning and Spaceborne Experiment in the Amazonas (BASE-A). *Journal of Geophysical Research*, 97, D13, 14581-14599.

Kaufman, Y. J., Remer, L. A., Ward, D. E., Kleidman, R., Flynn, L., Shelton, G., Ottmar, R. D., Li, R. -R., Fraser, R. S., McDougal, D., 1996. Relationship between remotely sensed fire intensity and rate of emission of smoke: SCAR-C Experiment. In J. S. Levine (Ed.), Global biomass burning: Atmospheric, climatic and biospheric implications (pp. 685-696). Cambridge: MIT Press.

Kaufman, Y. J., Justice, C. O., Flynn, L., Kendall, J. D., Prins, E. M., Giglio, L., Ward, D. E., Menzel, W. P., Setzer, A. W., 1998a. Potential global fire monitoring from EOS-MODIS. *Journal of Geophysical Research*, 103, 32, 215-32, 238.

Kaufman, Y. J., Kleidman, R. G., King, M. D., 1998b. SCAR-B fires in the tropics: properties and remote sensing from EOS-MODIS, *Journal of Geophysical Research*, 103, 31, 955-31, 968.

Li, X.; Christopher, S. A.; Chou, J.; Welch, R. M., 2000. Estimation of shortwave direct radiative forcing of biomass burning aerosols using angular dependence models. Journal of Applied Meteorology, v. 39, n. 12, p. 2278-2291.

Nobre, C. A.; Sellers, P. J.; Shukla, J., 1991. Amazonian deforestation and regional climate change. *J. Clim*., 4, 957-988.

Nobre, C. A.; Mattos, L. F.; Dereczynski, C. P.; Tarasova, T. A.; Trosnikov, I. V., 1998. Overview of atmospheric conditions during the smoke, clouds and Radiation-Brazil (SCAR-B) field experiment. Journal of Geophysical Research, v. 103, n. D31, p. 809-820.

Pereira, G.; Freitas, S. R.; Moraes, E. C.; Ferreira, N. J.; Shimabukuro, Y. E.; Rao, V. B.; Longo, K.M., 2009. Estimating trace gas and aerosol emissions over South America: Relationship between fire radiative energy released and aerosol optical depth observations, Atmospheric Environment, v. 43, p. 6388-6397.

Reid, J. S.; Hobbs, P. V.; Ferek, R. J., 1996. Physical and chemical characteristics of biomass burning aerosol in Brasil. In: SCAR-B Proceedings. São José dos Campos, Transtec editorial: 1996. p.165-169.

Reid, J. S.; Eck. T. F.; Christopher, S. A.; Hobbs, P.; Holben, B., 1999. Use of the Angstrom Exponent to Estimate the Variability of Optical and Physical Properties of Aging Smoke Particles in Brazil. Journal of Geophysical Research-Atmospheres, v.104, n. D22, p. 27473-27490.

SPRING. 2005. Sistema de Processamento de Informações Georreferenciadas. Versão 4.3. Instituto Nacional de Pesquisas Espaciais (INPE.

Tarasova, T. A.; Nobre, C. A.; Holben, B. N.; Eck, T. F.; Setzer, A., 1999. Assessment of smoke aerosol impact on surface solar irradiance measured in the Rondonia region of Brazil during smoke, cloud and radiation – Brazil. Journal of Geophysical Research, v. 104, D19, p. 161-170.

Tarasova, T. A.; Nobre, C. A.; Holben, B. N.; Eck, T. F.; Setzer, A., 2000. Modeling of gaseous, aerosol and cloudiness effects on surface solar irradiance measured in Brazil´s Amazonia 1992 - 1995. Journal of Geophysical Research, v. 105, D26, p. 961-969.

Tarasova, T. A.; Eck, T. F., 2000. Improvements in the broadband radiative transfer code aimed to achieve better agreement between modeled and measures solar irradiances on the ground**.** Proceedings of IRS' 2000. St. Petersburg, Russia,

Wagner, F.; Müller, D.; Ansmann, A., 2001. Comparison of the radiative impact of aerosols derived from vertically resolved (lidar) and vertically integrated (Sun photometer) measurements: Example of an Indian aerosol plume. Journal of Geophysical Research-Atmospheres, v. 106, n. D19, p. 22861-22870.

Wang, M., Howarth, P. J., 1993. Modeling errors in remote sensing image classification. Remote Sensing of Environment, v. 45, Issue 3, p. 261-271.